Live imaging of mammalian retina: rod outer segments are stained by conventional mitochondrial dyes

Paolo Bianchini*
University of Genoa
Laboratory for Advanced
Microscopy, Bioimaging, and Spectroscopy (LAMBS)
MicroSCoBiO Research Center
Department of Physics
Via Dodecaneso 33
16146, Genoa, Italy

Daniela Calzia*
Silvia Ravera*
University of Genoa
Department of Biology
V.le Benedetto XV 3
16132 Genova, Italy

Giovanni Candiano
G. Gaslini Children Hospital
Laboratory on Pathophysiology of Uraemia
L.go G. Gaslini 5
16147 Genova, Italy

Angela Bachi
San Raffaele Scientific Institute
Dipartimento di Biotecnologie (DIBIT)
Via Olgettina 60
20132 Milano, Italy

Alessandro Morelli
University of Genoa
Department of Biology
V.le Benedetto XV 3
16132 Genova, Italy

Maurizio Bruschi
G. Gaslini Children Hospital
Laboratory on Pathophysiology of Uraemia
and
RenalChild Foundation
L.go G. Gaslini 5
16147 Genova, Italy

Isidoro M. Pepe
University of Genoa
Department of Biology
V.le Benedetto XV 3
16132 Genova, Italy

Alberto Diaspro
University of Genoa
Laboratory for Advanced
Microscopy, Bioimaging, and Spectroscopy (LAMBS)
MicroSCoBiO Research Center
Department of Physics
Via Dodecaneso 33
16146, Genoa, Italy
and
Fondazione Italiana per la Ricerca sul Cancro (FIRC)
Institute for Molecular
Oncology, Istituto Firc di Oncologia Morelcolare (IFOM)
Via Adamello, 16
20139 Milan, Italy

Isabella Panfoli
University of Genoa
Department of Biology
V.le Benedetto XV 3
16132 Genova, Italy

Abstract. The vertebrate retina is an array of "narrow-capture" photoreceptive elements of diverse cellular types that allow the fine spatial resolution characteristic of vision. Imaging of photoreceptors and of the whole retina has been previously reported; however, both were achieved exclusively after fixation. We report our development of a new technique for imaging live bovine retinas *ex vivo*. Using this technique, we conducted fluorescence confocal laser scanning microscopic imaging of bovine retinas. Eyecups were incubated with conventional fluorescent mitochondrial probes (MitoTracker and JC-1). Unexpectedly, we found that, besides the retinal mitochondria, the rod outer segments that are devoid of mitochondria were also stained. No other neuron was stained. Both protonophores, which decrease mitochondrial membrane potential, or inhibit electron transport strongly inhibited the selective association of dyes with both retinal rod outer segments and mitochondria. This is the first time that living rod outer segments were visualized by this technique. This finding may shed light on previous reports of the existence of a proton potential across the disk membranes and on the mechanism of the adenosine tri-phosphate (ATP) supply for phototransduction, which still requires investigation. [DOI: 10.1117/1.2982528]

Keywords: confocal laser scanning microscopy; fluorescent dyes; mitochondrial probes; retina; imaging; JC-1; MitoTracker.

Paper 08068R received Feb. 26, 2008; revised manuscript received Apr. 29, 2008; accepted for publication May 2, 2008; published online Oct. 14, 2008.

1 Introduction

The retina comprises cells from the central nervous system (CNS) for the transduction of light messages into electrical signals.[1–3] The photoreceptors (rods and cones) are the sites of light capture,[4] while the retinal physiological repertoire is due to downstream diverse inner-retinal neurons.[3]

The rods, where photoreception in dim light begins,[3,5,6] consist of a rod inner segment (RIS) and a rod outer segment (ROS). The RIS contains the nucleus and other organelles. The ROS is composed of a stack of sealed, flattened membrane vesicles—the disks—that contain the photopigment rhodopsin (Rh) and are surrounded by the plasma membrane. The ROS is constantly renewed;[7,8] new disks are formed at the cilium of the outer segment from evaginations of the plasma membrane and are displaced toward the apical tip, where old disks are shed by the rod pigmented epithelium

*Paolo Bianchini, Daniela Calzia and Silvia Ravera contributed equally to this work.
Address all correspondence to Isabella Panfoli, DIBIO, University of Genova, V. le Benedetto XV, 3 - Genoa, 16132 Italy; Tel: +39 010 3537397; Fax: +39 010 3538153; E-mail: Isabella.Panfoli@unige.it

1083-3668/2008/13(5)/054017/6/$25.00 © 2008 SPIE

(RPE).[8,9] In past years we have investigated adenosine triphosphate (ATP) production in the ROS.[10] Recently, we reported a new protocol for the imaging of disks for immunofluorescence confocal laser scanning microscopy (CLSM),[11] and the first comprehensive proteomic analysis of purified rod disks, which were obtained by combining the results of 1-D or 2-D gel electrophoresis separation of disk proteins to matrix-assisted laser desorption/ionization–time-of-flight (MALDI-TOF) or liquid chromatography electrospray ionisation tandem mass spectrometry (nLC-ESI-MS/MS) mass spectrometry techniques. Proteins involved in vision as well as in aerobic metabolism were found, among which were the five complexes of oxidative phosphorylation.[12]

Several studies have addressed the immunohystochemical analysis of the retina, mostly by inclusion or on previously fixed tissue.[13] For example, the retinal histoarchitecture was recently evaluated by light microscopy on sections of the inferior portion of the eye wall, fixed and embedded in epoxy resin.[14] CLSM was also employed to analyze the structure of isolated mammalian retinas by immunocytochemical analyses,[15] but this technique was applied only to fixed retinas with the exclusion of vital dyes.[16] A technique for corneal confocal microscopy imaging (Retina Tomograph II Rostock Cornea Module) was developed.[17] Retinal *in vivo* studies were conducted mainly for noninvasive diagnostic scope by scanning-laser ophthalmoscopy (SLO),[18,19] optical coherence tomography (OCT),[20,21] and optical Doppler tomography (ODT).[22]

Permeant cationic lipophylic dyes have been employed for the investigation of mitochondrial membrane potential and intracellular distribution, by both regular microscopy and CLSM.[23] In fact, these probes, which are essentially carbocyanine and rhodamines, show a potential-dependent partitioning across highly polarized mitochondrial membranes. These techniques allow the imaging of mitochondria in living cells to obtain useful information on both mitochondrial morphology and cellular functionality.

In this paper we describe a new technique aimed at imaging the mitochondria of a living retina. We developed a new *ex vivo* technique that allows the morphologic and functional characteristics of the posterior eyecup to remain virtually unchanged. A CLSM imaging study of whole bovine retinas was conducted that employed two lipophylic fluorescent vital mitochondrial dyes, namely MitoTracker Deep Red 633 (MT Deep Red) and JC-1. Treatments were performed by incubating probes in the living eye-semicup retinas. Then the imaging was performed by mounting either the eye semicups or retinas onto a coverslip chamber. By using this procedure, we could image not only the mitochondria of the various retinal cell types, but also the ROS. Such unexpected staining was quite surprising in that it seemed specific, being inhibited by inhibitors of mitochondrial respiration or protonophores.

2 Materials and Methods

2.1 *Materials*

Mitochondrial fluorescent probes, MT Deep Red and JC-1, were obtained from Invitrogen (Carlsbad, California). Salts, respiratory chain inhibitors (rotenone, antimycin A), nigericin, and all other chemicals were purchased from Sigma-Aldrich (St. Louis, Missouri). Ultrapure water (Milli-Q; Millipore, Billerica, Massachusetts) was used throughout the study. Safety precautions were taken for chemical hazards from carrying out the experiments as described below.

2.2 *Retinal Preparations*

Freshly enucleated bovine eyes were obtained from a local slaughterhouse within 1.5 hr of animal death. Eyes were cut in half and the eyeballs divided into two eyecups. The cornea, vitreous, and lens were removed. The semicup containing the retina and choroid was incubated for 15 min in a mammalian ringer (MR), consisting of 0.157 M NaCl, 5 mM KCl, 7 mM Na_2HPO_4, 8 mM NaH_2PO_4, 0.5 mM $MgCl_2$, and 2 mM $CaCl_2$ with a 6.9 pH, in the presence of a protease inhibitor cocktail (Sigma-Aldrich, St. Louis, Missouri) and ampicillin (100 μg/ml) in dim red light.

2.3 *Probe Staining*

Probe incubation of the retinas, still attached to the rear portion of the eye wall, was conducted directly in the eye semicups. The mitochondrial dyes MT Deep Red and JC-1 were dissolved in dimethylsulfoxide (DMSO) to make 200-μM stock solutions, which were kept at −20 °C in dark bottles. Staining solutions were prepared immediately before use by adding the dye stock solution to MR in the eye semicups. About 9 ml of MR containing 2 mM glucose and the mitochondrial vital dyes MT Deep Red (500 nM) and JC-1 (4.6-μM final concentration). These steps were performed in dim red light. Glucose was freely taken up by neurons of the retina thanks to the presence of specific transporters, such as GLUT-1 in the rods.[24]

After about 20 min of incubation, the rods spontaneously detached from the RPE, so the retinas were easily removed from the eye semicups and mounted on coverslip glass for CLSM. Alternatively, the whole posterior eye semicup was cut at the edge and mounted over the microscope immersion objective by a homemade arrangement. Samples were not fixed or washed.

To test the specificity of Mitotracker staining, classical respiratory chain inhibitors such as. 10-μM rotenone and 10-μM antymicin A (Sigma-Aldrich, St. Louis, Missouri) were added to the probe incubation solution. A protonophore, 4-μM nigericin, was added directly onto the retinas during JC-1 confocal microscopy measurements.

2.4 *Confocal Laser Scanning Microscopy (CLSM)*

CLSM imaging was performed on the above samples at 23 °C. The measurements were acquired by means of a Leica TCS SP5-AOBS (Leica Microsystems, Mannheim, Germany) inverted confocal laser scanning microscope equipped with 457, 476, 488, 514, 543, and 633-nm laser lines. Specimens were normally examined with an HCX APO L U-V-I 63 ×/0.9 NA (Leica Microsystems, Mannheim, Germany) water immersion objective with a working distance of 2.2 mm. This objective guaranteed a good balance between confocal sectioning and penetration depth.[25] The retinas were either left in the eye semicup or detached from the choroid. In the former case, the whole semicup was cut at the rim and mounted onto the coverslip chamber. In the latter case the whole semicup was immersed in a small pool arranged around the objective. Using this setup, it was possible to hold the eye semicup,

meanwhile, the objective was free to move up and down to reach the proper focal planes. This procedure was adopted when incubation was longer than 10 min, because in this case the retina detached spontaneously from the RPE. No differences were noted in either procedure.

Retinas stained with MT Deep Red were excited at 633 nm, and the emission was collected in the spectral range from 650 to 700 nm. The laser power and detection settings were kept equal in all the experiments to avoid artifacts and allow comparison of retinas treated or not with inhibitors. Retinas stained with JC-1, as already described, were excited at 488 nm. The emission was collected by a sequential scan in two channels, using the same detector at the same gain power and moved sequentially through the spectral range, with the green one (520 ± 20 nm) and the red one (580 ± 20 nm) representing the monomer and the J-aggregate fluorescence, respectively. The derivation of the ratio of the monomer to the aggregate fluorescence provided a measure directly related to the membrane potential.

The resulting images were acquired, stored, and visualized with Leica Confocal Software (LCS, Leica Microsystems, Mannheim, Germany). Image elaboration, analysis, and 3-D rendering were realized by Image J software (U. S. National Institutes of Health, Bethesda, Maryland).

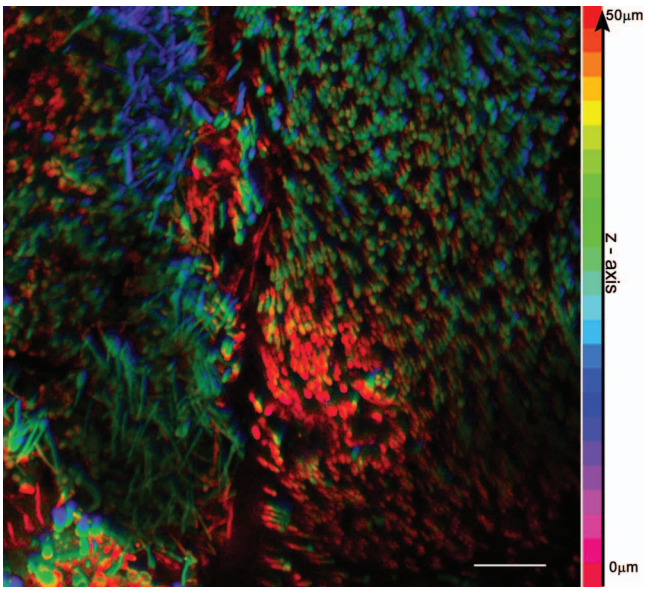

Fig. 1 Color-coded 3-D projection of MT Deep Red fluorescence in a living bovine retina. The color table translates the colors into the relative z depth of the image. The scale bar is 30 μm.

3 Results and Discussion

Many lipophylic fluorescent probes interact with actively respiring membranes and show changes in their fluorescent characteristics as they redistribute between compartments. We employed MT Deep Red and JC-1 to image the mitochondria of a whole retina by a new *ex vivo* approach. The novelty of the procedure is in the treatment of the samples, which maintains the physiological and morphological features of the eye, and in the possibility of imaging a living retina. Eye semicups from freshly detached bovine eyes, with the retinas still attached to the RPE, were filled with MR containing 1 mM glucose, 50 μg/ml ampicillin, and a protease inhibitor cocktail, then incubated for 10 min. Then probes were added to the solution and it was incubated for 15 min more. Finally, the retinas, which by this time had spontaneously detached from the RPE, were not fixed or washed and were mounted on the coverslips.

Figure 1 shows a CLSM color-coded 3-D projection of MT Deep Red fluorescence of a portion of a whole bovine living retina, treated as described above. MT Deep Red is a photostable permeant cationic fluorescent mitochondrial probe,[26] that is known to be taken up by functional mitochondria, due to their high membrane potential, without fluorescence quenching. The figure shows that, quite unexpectedly, fluorescence appears to be distributed on the ROS. The morphology of the ROS is clear enough to allow unambiguous identification of its structures.[27,28] Moreover, considering the relative z depth of the picture as translated by the color table, the ROS structures appear fluorescent for about 30 μm, i.e., a half of their length, which is 60 μm (with 1.2-μm mean diameter in the cattle[27,28]). Interestingly, the ROS distal tract is known to be active in phototransduction, thanks to the modified composition of disk lipids.[29,30]

Figure 2 contains CLSM images showing the fluorescence of MT Deep Red in representative portions of a whole bovine living retina. In Fig. 2(a), both the mitochondria belonging to other retinal cell types and some detached ROS structures are visible. The different mitochondrial fluorescence intensities may represent variable planes of focus. In fact, mitochondria undulate in and out of the plane of observation. Variations in the mitochondrial accumulation of cationic probes were reported to be potential-dependent.[23] Figure 2(c) shows a portion of a whole retina with fluorescent rods still attached that seem to be imaged in perspective from their apical zone, as judged by the absence of mitochondria on the plane nearer to the objective. No other neurons of the retina were visible in the many pictures acquired from the imaged whole retinas. MT Deep Red ROS fluorescence appears to be more intense in the apical tract of the ROS, which is functional in phototransduction.[29,30] The objects shown in Fig. 2(b), are the 3-D reconstructions of a part of the fluorescent tips in Fig. 2(c), as determined by an Image J software plug-in.

Impairment of mitochondrial function with inhibitors of electron transport in the respiratory chain is known to cause a decrease of MT Deep Red fluorescence in mitochondria. To verify the specificity of the ROS staining, in a parallel set of experiments we exposed the living retinas to both rotenone, a specific inhibitor of NADH dehydrogenase (complex I of the respiratory chain) and antimycin A, an inhibitor of complex III of the respiratory chain, before adding fluorescent probes. Inhibitors (10-μM final concentration, each) were added to the MR in the eye semicup 5 min after the start of incubation. MT Deep Red was added 5 min later, and after 15 more min, the retinas were imaged. Figure 2(d) shows that, when preincubated in the presence of rotenone and antimycin-A, the MT Deep Red fluorescence intensity in the ROS was reduced by 4 to 5 fold, as evaluated by densitometric quantitation performed using the Image J 1.31 v. software. Quantification was performed to compare the mean relative optical density value calculated for five identical areas of each image after subtraction of the mean background value for each. Accordingly, a

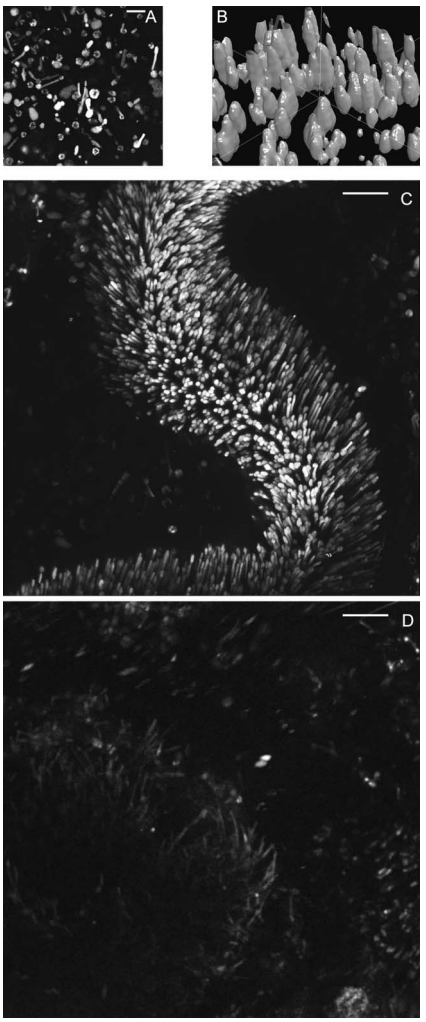

Fig. 2 CLSM images of MT Deep Red fluorescence in a living bovine retina. All the scale bars are 30 μm. (A) Mitochondria of the various cell types of the retina and some detached ROS are clearly visible. (B) 3-D reconstruction made on a portion of the image stack visualized in panel C. (C) Maximum projection (z=84 μm) of serial confocal sections on an undulate part of the retina. (D) Maximum projection (z =52 μm) of serial confocal sections of an undulate part of the retina after preincubation in the presence of rotenone and antimycin-A.

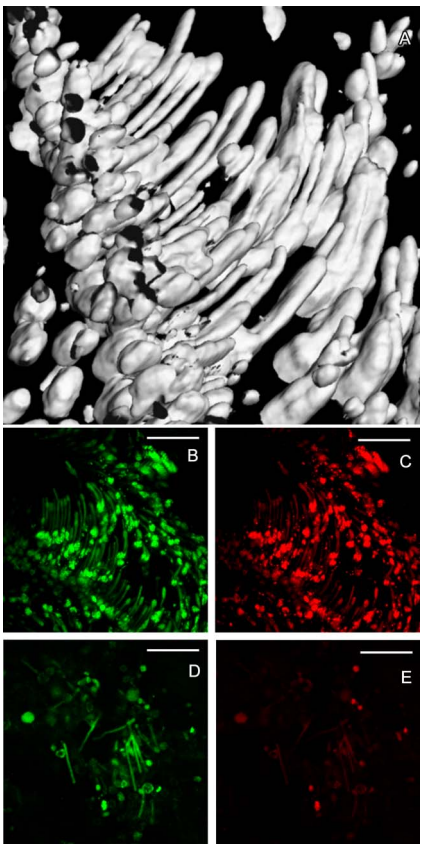

Fig. 3 CLSM images of JC-1 fluorescence in a living bovine retina. All the scale bars are 30 μm. (A) 3-D reconstruction made on a portion of the image stack visualized in panel B. (B)–(C) Maximum projection (z=54 μm) of serial confocal sections on an undulate part of the retina. Green (520±20 nm) and red (580±20 nm) channels were acquired sequentially. (D)–(E) Maximum projection (z=54 μm) of serial confocal sections on an undulate part of the retina 10 min after the addition of nigericin. Green (520±20 nm) and red (580±20 nm) channels were acquired sequentially. (Color online only.)

decrease in MT Deep Red fluorescence was observed in mitochondria [Fig. 2(d)]. MT Deep Red probes are known to passively diffuse across the plasma membrane and accumulate permanently in actively respiring mitochondria.[26] The fluorescence intensity associated with a membrane is likely to be a reflection of a protonic potential because, at least in mitochondira, the electron transport establishes a proton gradient across the mitochondrial inner membrane.

The unexpected staining of ROS prompted us to try another classical mitochondria-specific dye to verify whether the phenomenon was repeatable. We turned to JC-1, a membrane-potential carbocyanine-sensitive probe for imaging living cells. The advantage of JC-1 over rhodamines is that its color alters reversibly from green to red with increasing membrane potential. The so-called J-aggregates are favored at a higher membrane potential. Figure 3 shows the results of an experiment in which a whole retina was incubated with JC-1 by the same procedure as used in Figs. 1 and 2. CLSM images in Figs. 3(b)–3(e) show that both the ROS and mitochondria of the various retinal cells appear fluorescent (10 min after addition of JC-1). Figure 3(a) shows a 3-D reconstruction of the image in Figs. 3(b) and 3(c), which show the green and red fluorescence of JC-1, respectively, in the two different channels acquired sequentially. In the ROS, the dye underwent a change in fluorescence emission from green to red. In inactive mitochondria, the JC-1 monomer emits green fluorescence, while the aggregated form, which is prevalent when membrane potential (i.e., functional capacity) is high, emits a red fluorescence. J-aggregate fluorescence intensity was found to increase linearly with increasing mitochondrial membrane potential.[31,32] Compared to other dyes that give single-component fluorescence signals, JC-1 red fluorescence is not affected by mitochondrial size, shape, or density.[33] J-aggregate fluorescence was demonstrated to be independent of pH, within the physiological range, and not to be due to any metabolic conversion.[32] In experiments with mitochondria, the red peak was found to be sensitive to protonophores,[32] which cause a loss of membrane potential; thus, we utilized nigericin, a specific protonophore, to verify

whether the ROS behaved the same as mitochondria. Nigericin was added directly to the imaged retina on the glass slide during the CLSM experiment (at a 4-μM final concentration in a minimum-DMSO volume), then the observation of the retina was continued. Fluorescence in the sample was found to diminish, both in the ROS and in most of the mitochondria: Figs. 3(d) and 3(e) show that 10 min after the addition of nigericin, the red fluorescence was reduced by 2 to 3 fold, as shown in Fig. 3. On the other hand, green fluorescence persisted, since the sample was not processed further. The large aggregates present in Figs. 3(a)–3(c), likely due to a relatively high potential on the ROS tips, disappeared with the addition of nigericin. Since JC-1 does not exhibit any concentration-dependent quenching effects,[32] a strong shift from red to green emission of JC-1 should correspond to a decrease in membrane potential.

By the technique reported herein, only the ROS and mitochondria appear to be stained by fluorescent mitochondrial probes in a whole living retina. The same results were obtained when the whole eye semicup was mounted onto the coverslip (data not shown). No differences were observed, such as those for the fluorescence emission intensity, when the incubation with both dyes was conducted in room light with respect to dim red light (data not shown).

4 Conclusion

This paper demonstrated that the mitochondria-specific interaction of the cationic dyes utilized in this study depended on the presence of a high transmembrane potential, like the proton gradient $[\Delta\mu(H^+)]$ maintained by functional mitochondria across the inner membrane. In our experimental conditions, dissipation of membrane potential by treatment with mitochondrial poisons and uncouplers eliminated the selective association of MT Deep Red and JC-1 with both the mitochondria and the ROS (Figs. 2 and 3). Further studies may establish whether this means that the tip of the ROS possesses a transmembrane potential of the kind and order of magnitude as those of mitochondria (about 190 mV) and an electron transport. For our CLSM measurements, the eye semicups were incubated with the probes in the dark, then retinas were withdrawn and mounted onto the glass slide in room light. In these conditions, the ROS should be in a relatively hyperpolarized state. If the high transmembrane potential to which JC-1 is sensitive resides on the ROS plasmamembrane, the whole ROS would be stained, which seems not to be the case. On the other hand, it may be supposed that the high potential resides in the disk membranes. Several previous results are consistent with the notion of ROS disks as organelles able to store and/or release protons.[34,35] The existence of a $\Delta\mu(H^+)$ across the disk membranes was previously demonstrated by light scattering experiments.[36,37] According to these authors, the light-scattering signal also suggested a H^+ translocation across disks. It is tempting to assume that a $\Delta\mu(H^+)$ across disk membranes is responsible for the JC-1 staining (Fig. 3), because it was reverted by the protonophore nigericin.

In mitochondria, membrane potential ($\Delta\psi$) represents a sensitive parameter of the coupling of the mitochondrial bioenergetic function. Moreover, increases in the accumulation of cationic mitochondrial probes were suggested to reflect an increase in ATP requirement in cells.[38] The ROS is considered to contain organelles devoid of mitochondria, the site of anaerobic metabolism, even though glycolysis, which is present in the ROS, was estimated to be insufficient to supply ATP for phototransduction.[6,39] The results shown in this paper suggest that the functioning of rod disks might involve the build-up of a proton potential. This would be consistent with our recent results from a proteomic analysis of purified disks, where the proteins of the four complexes of the electron transport chain were found to be expressed.[12] Moreover, those results showed that F_1F_o-ATP synthase is located and catalytically active in the ROS disk membranes,[12] suggesting the presence of an aerobic glucose metabolism in disk membranes that could represent a mechanism for an ATP supply in phototransduction. Further studies may clarify the physiological reason for the ROS behavior when exposed *ex vivo* to classical vital mitochondrial dyes.

Acknowledgments

The authors thank Prof. Pietro Calissano (University of Roma, Italy), Prof. Rosanna Gusmano (RenalChild Foudation, Gaslini Hospital, Genova, Italy), and Prof. Bruno Andrea Melandri (University of Bologna, Italy) for their invaluable contributions. This work was supported by grants from the Italian Ministry for Research and Technology (MIUR). For A. Diaspro and P. Bianchini, this work was granted by Istituto Firc di Oncologia Morelcolare (IFOM), Milan; PRIN2006; the Italian Research Program of National Interest 2006 (2006028909); and the Fondazione San Paolo (Torino, Italy). For M. Bruschi, this work was granted by the RenalChild Foundation.

References

1. R. W. Rodieck, "The primate retina," Vol. **4** in *Comparative Primate Biology, Neurosciences*, H. D. Steklis and J. Erwin, Eds., pp. 203–278, Alan R. Liss, New York (1988).
2. P. Sterling, "Retina" in *The Synaptic Organization of the Brain*, G. M. Shepherd, Ed., pp. 170–213, Oxford University Press, New York (1990).
3. R. H. Masland, "Neuronal diversity in the retina," *Curr. Opin. Neurobiol.* **11**, 431–436 (2001).
4. K. D. Ridge, N. G. Abdulaev, M. Sousa, and K. Palczewski, "Phototransduction: crystal clear," *Trends Biochem. Sci.* **28**, 479–487 (2003).
5. L. Stryer, "Vision: from photon to perception," *Proc. Natl. Acad. Sci. U.S.A.* **93**, 557–559 (1996).
6. I. M. Pepe, "Recent advances in our understanding of rhodopsin and phototransduction," *Prog. Retin Eye Res.* **20**, 733–759 (2001).
7. D. Bok, "Retinal photoreceptor-pigment epithelium interactions," Friedenwald lecture, *Invest. Ophthalmol. Visual Sci.* **26**, 1659–1694 (1985).
8. R. W. Young, "Shedding of discs from rod outer segments in the rhesus monkey," *J. Ultrastruct. Res.* **34**, 190–203 (1971).
9. S. C. Finnemann, V. L. Bonilha, A. D. Marmorstein, and E. Rodriguez-Boulan,"Phagocytosis of rod outer segments by retinal pigment epithelial cells requires alpha (v) beta 5 integrin for binding but not for internalization," *Proc. Natl. Acad. Sci. U.S.A.* **94**, 12932–12937 (1997).
10. I. M. Pepe, L. Notari, C. Cugnoli, I. Panfoli, and A. Morelli, "ATP synthesis in the disk membranes of rod outer segments of bovine retina," *J. Photochem. Photobiol., B* **66**, 148–152 (2002).
11. S. Ravera, D. Calzia, P. Bianchini, A. Diaspro, and I. Panfoli, "Confocal laser scanning microscopy of retinal rod outer segment intact disks: new labeling technique," *J. Biomed. Opt.* **12**, 050501 (2007).
12. I. Panfoli, L. Musante, A. Bachi, S. Ravera, D. Calzia, A. Cattaneo, M. Bruschi, P. Bianchini, A. Diaspro, A. Morelli, I. M. Pepe, C. Tacchetti, and G. Candiano, "Proteomic analysis of the retinal rod outer segment disks," *J. Proteome Res.* (in press).

13. L. Vitanova, S. Haverkamp, and H. Wässle, "Immunocytochemical localization of glycine and glycine receptors in the retina of the frog Rana ridibunda," *Cell Tissue Res.* **317**, 227–235 (2004).
14. A. K. Junk, A. Mammis, S. I. Savitz, M. Singh, S. Roth, S. Malhotra, P. S. Rosenbaum, A. Cerami, M. Brines, and D. M. Rosenbaum, "Erythropoietin administration protects retinal neurons from acute ischemia-reperfusion injury," *Proc. Natl. Acad. Sci. U.S.A.* **99**, 10659–10664 (2002).
15. S. Haverkamp and H. Wässle, "Immunocytochemical analysis of the mouse retina," *J. Comp. Neurol.* **42**, 1–23 (2000).
16. N. Cueca, I. Pinilla, Y. Sauvé, and R. Lund, "Early changes in synaptic connectivity following progressive photoreceptor degeneration in RCS rats," *Eur. J. Neurosci.* **22**, 1057–1072 (2005).
17. V. Iordanidou, G. Sultan, C. Boileau, M. Raphael, C. Baudouin, and Marfan Study Group, "*In vivo* confocal microscopiy in marfan syndrome," *Cornea* **26**, 787–792 (2007).
18. M. W. Seeliger, S. C. Beck, N. Pereyra-Muñoz, S. Dangel, J. Y. Tsai, U. F. Luhmann, S. A. van de Pavert, J. Wijnholds, M. Samardzija, A. Wenzel, E. Zrenner, K. Narfström, K. E. Fahl, N. Tanimoto, and F. Tonagel, "*In vivo* confocal imaging of the retina in animal models using scanning laser ophthalmoscopy," *Vision Res.* **45**, 3512–3519 (2005).
19. A. Maass, P. L. von Leithner, V. Luong, L. Guo, T. E. Salt, F. W. Fitzke, and M. F. Cordeiro, "Assesment of rat and mouse RGC apoptosis imaging *in vivo* with different scnning laser ophthalmoscopes," *Curr. Eye Res.* **32**, 851–861 (2007).
20. V. J. Srinivasan, M. Wojtkowski, J. G. Fujimoto, and J. S. Duker, "*In vivo* measurement of retinal physiology with high-speed ultrahigh-resolution optical coherence tomography," *Opt. Lett.* **31**, 2308–2310 (2006).
21. C. C. Rosa, J. Rogers, J. Pedro, R. Rosen, and A. Podoleanu, "Multiscan time-domain optical coherence tomography for retina imaging," *Appl. Opt.* **1**, 1795–1808 (2007).
22. Z. G. Wang, C. Lee, W. Waltzer, Z. J. Yuan, Z. L. Wu, H. K. Xie, and Y. T. Pan, "Optical coherence tomography for noninvasive diagnosis of epithelial cancers," *Proc. IEEE Eng. Med. Biol. Soc.* **1**, 129–132 (2006).
23. M. Poot, Y. Zhang, J. A. Kramer, S. Wells, L. J. Jones, D. K. Hanzel, A. G. Lugade, V. L. Singer, and R. P. Haugland, "Analysis of mitochondrial morfology and function with novel fixable fluorescent stains," *J. Histochem. Cytochem.* **44**, 1363–1372 (1996).
24. S. C. Hsu and R. S. Molday, "Glycolytic enzymes and a GLUT-1 glucose transporter in the outer segments of rod and cone photoreceptor cells," *J. Biol. Chem.* **266**, 21745–21752 (1991).
25. A. Diaspro, *Confocal and Two-Photon Microscopy*, Wiley-Liss, Inc., New York (2002).
26. O. Uckermann, I. Iandiev, M. Francke, K. Franze, J. Grosche, S. Wolf, L. Kohen, P. Wiedemann, A. Reichenbach, and A. Bringmann, "Selective staining by vital dyes of Müller glial cells in retinal wholemounts," *Glia* **45**, 59–66 (2004).
27. T. Norisuye, W. F. Hoffman, and H. Yu, "Intact photoreceptor membrane from bovine rod outer segment: size and shape in bleached state," *Biochemistry* **15**, 5678–5682 (1976).
28. S. Nickell, P. S. Park, W. Baumeister, and K. Palczewski, "Three-dimensional architecture of murine rod outer segments determined by cryoelectron tomography," *J. Cell Biol.* **177**, 917–925 (2007).
29. K. Boesze-Battaglia and A. D. Albert, "Cholesterol modulation of photoreceptor function in bovine retinal rod outer segment," *J. Biol. Chem.* **265**, 20727–20730 (1990).
30. A. D. Albert and K. Boesze-Battaglia, "The role of cholesterol in rod outer segment membranes," *Prog. Lipid Res.* **44**, 99–124 (2005).
31. L. B. Chen, "Mitochondrial membrane potential in living cells," *Annu. Rev. Cell Biol.* **4**, 155–181 (1988).
32. M. Reers, T. W. Smith, and L. B. Chen, "J-aggregate formation of carbocyanine as a quantitative fluorescent indicator of membrane potential," *Biochemistry* **30**, 4480–4486 (1991).
33. R. L. Divi, K. J. Haverkos, J. A. Humsi, M. E. Shockley, C. Thamire, K. Nagashima, O. A. Olivero, and M. C. Poirier, "Morphological and molecular course of mitochondrial pathology in cultured human cells exposed long-term to Zidovudine," *Environ. Mol. Mutagen.* **48**, 179–189 (2007).
34. D. G. McConnell, C. N. Rafferty, and R. Dilley, "The light-induced proton uptake in bovine retinal outer segment fragments," *J. Biol. Chem.* **243**, 5820–5826 (1968).
35. U. B. Kaupp, P. P. Schnetkamp, and W. Junge, "Rapid calcium release and proton uptake at the disk membrane of isolated cattle rod outer segments I: Stoichiometry of light-stimulated calcium release and proton uptake," *Biochemistry* **20**, 5500–5510 (1981).
36. R. Uhl, R. Zellmann-Kraska, and H. Desel, "Optical probes of intradiskal processes in rod photoreceptor I: Light-scattering study of ATP-dependent light reactions," *Photochem. Photobiol.* **3**, 529–548 (1979).
37. R. Uhl, R. Zellmann-Kraska, and H. Desel, "Optical probes of intradiskal processes in rod photoreceptor II: Light-scattering study of ATP-dependent light reactions," *Photochem. Photobiol.* **3**, 549–564 (1979).
38. L. V. Johnson, M. L. Walsh, B. J. Bockus, and L. B. Chen, "Monitoring of relative mitochondrial membrane potential in living cells by fluorescence microscopy," *J. Cell Biol.* **88**, 526–535 (1981).
39. S. C. Hsu and R. S. Molday, "Glucose metabolism in photoreceptor outer segments. Its role in phototransduction and in NAPH-requiring reactions," *J. Biol. Chem.* **269**, 17954–17959 (1994).